

The applicability of the holographic and speckle interferometries in the plate bending problem

ELŻBIETA JANKOWSKA

Institute of Physics, Technical University of Wrocław, Wybrzeże Wyspiańskiego 27, 50-370 Wrocław, Poland.

Both the holographic and speckle interferometries belong to non destructive optical methods, characterized by high accuracy of order of the light wavelength used. They are used to compare the images of the object before and after its deformation. The information about the changes in the object state is recorded in the form of differential fringes, whose shape, configuration and quantity play a fundamental role in the measurement interpretation. An essential limitation of the application range of both these methods is due to the restricted resolving power of the system used to analyse the differential interference image. This means that the image to be analyzed may not be covered with fringes spaced by the distance neither less than its limiting value following from the resolving power of the analyser (which is an upper bound restrictions), nor greater than the length of the examined object (which is a lower bound restriction).

If the examined object is of the length l the maximal number of distinguishable fringes n is

$$n_{\max} = \frac{l}{d_{\min}}, \quad (1)$$

where l — object length,

d_{\min} — least limiting spacing between two fringes. The quantity d_{\min} is influenced by the image graininess, the contrast of fringes and the quality of the analysing system.

The maximal quality of fringes is closely related to the maximal measurable translation w_{\max}

$$w_{\max} = n_{\max} \delta, \quad (2)$$

where δ is the value of the respective component of the translation deformation corresponding to the interfringe distance.

From the formula (2) it follows that the quantity influences the measurement range if it is assumed that n_{\max} is invariant for given measurement.

In this paper methods of holographic and speckling interferometry are compared, so far as the object translational deformation is concerned for the measuring geometry shown in Fig. 1.

In holographic interferometry the interfringe distance δ_{hol} is described by the relation [1]:

$$\delta_{\text{hol}} = \frac{\lambda}{2\cos\frac{\Theta}{2}} \approx \frac{\lambda}{2}, \quad (3)$$

where Θ — angle between the observation direction and the reference beam, rigorously determined for the given measurement system shown in Fig. 1.

In the speckle interferometry the quantity is defined by the formula

$$\delta_{\text{spec}} = \frac{\lambda mL}{2AU}, \quad (4)$$

in the form of differential fringes, whose shape, configuration and quantity play

where A – defocussing of the recording system,
 U – coordinate of the analysing aperture,
 m – magnification of the recording system,
 L – distance between the filtering lens and the aperture.

The formula (4) is employed in the examinations of the object bending [2–4], and may be changed by selecting suitably the geometry of both the recording and analysing systems (Fig. 2a, b.)

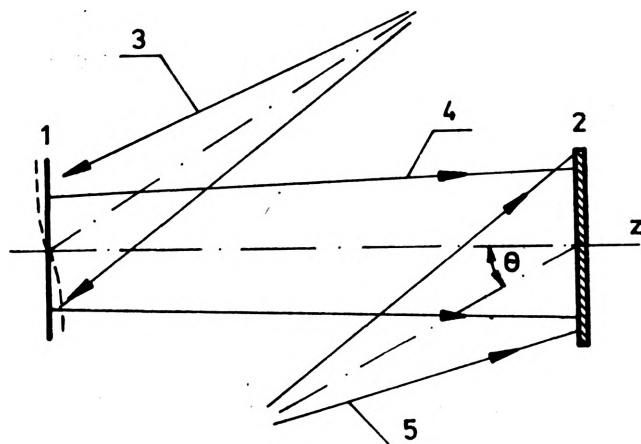


Fig. 1. Holographic interferometry – recording system: 1 – object, 2 – photoplate, 3 – illumination beam, 4 – object beam, 5 – reference beam

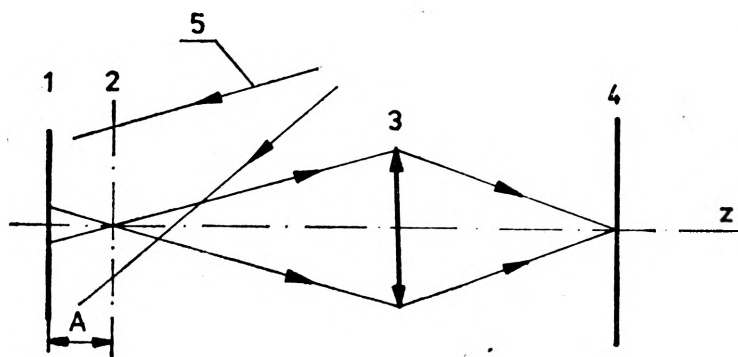


Fig. 2a. Speckle interferometry – recording system: 1 – object, 2 – focussing plane, 3 – recording lens, 4 – photoplate, 5 – illumination beam, A – defocussing of the recording system

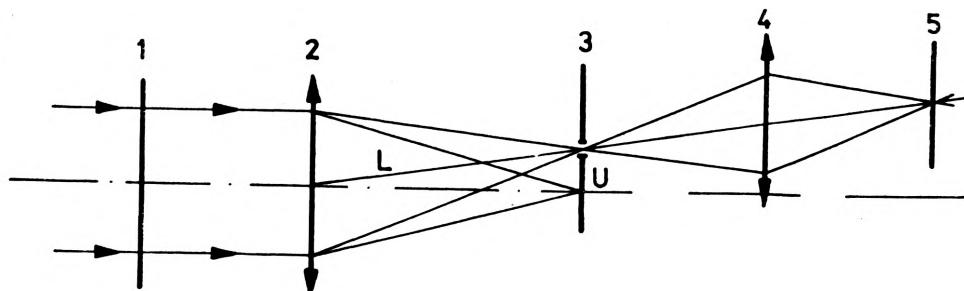


Fig. 2b. Speckle interferometry – reconstruction system: 1 – double exposed transparency, 2 – filtering lens, 3 – aperture plane, 4 – image lens, 5 – image plane, L – distance between the filtering lens and the aperture, U – coordinate of the analysing aperture

As it follows from the formula (2), the highest measured translation w may be increased by increasing δ . If we use a system for which

$$\delta_{\text{spec}} > \delta_{\text{hol}}, \quad (5)$$

i.e., that

$$\frac{mL}{AU} > 1, \quad (6)$$

then in the speckle method a greater object bending becomes recordable than it is the case in the holographic method for the same number of fringes. A suitable choice of parameters satisfying the condition (6) allows to change the measurement range of the method and to examine the bendings, which may not be recorded by using holographic methods.

An example

A comparison of both the methods have been carried out by testing the bending of a circular plate with an aperture, the plate being fastened at its periphery and loaded with a concentrated force. The scheme of the loading and the plate holder is shown in Fig. 3.

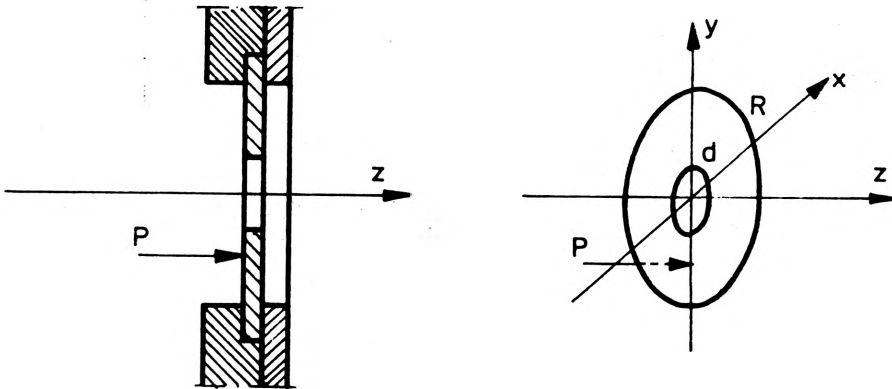


Fig. 3. Schematic diagram of the loading and the plate holder: P – concentrated force, R – radius of the plate, d – radius of the aperture

The measurements based on speckling interferometry method have been carried out by using an argon laser of the wavelength $\lambda = 0.5145 \cdot 10^{-3}$ nm. The recordings of analysis have been performed for the following parameters: $m = 7.669$, $L = 490$ mm, $A = 100$ mm, $U = 90$ mm. The maximal number of fringes, which may be observed when analysing visually the plate have been calculated from the formula (1). For the calculations the value of d_{min} was assumed to be equal to 0.635 nm (this value follows from the resolving powers of the eye and the geometry of the analysing system). The object diameter was 70 mm. The maximal plate bending recordable by the holographic method calculated from the formula (2), was $w_{\text{max}} = 28.14$ μm .

The application of the speckling method allowed to measure the comparable bending $w = 27.4$ μm , while the number of fringes (only six) contained in the interference pattern was 17 times less than the number of fringes appearing in the holographic method for the same plate bending. This is due to a suitable selection of the optical system parameters in the speckling method, which determine the value of δ_{spec} (formula (4)).

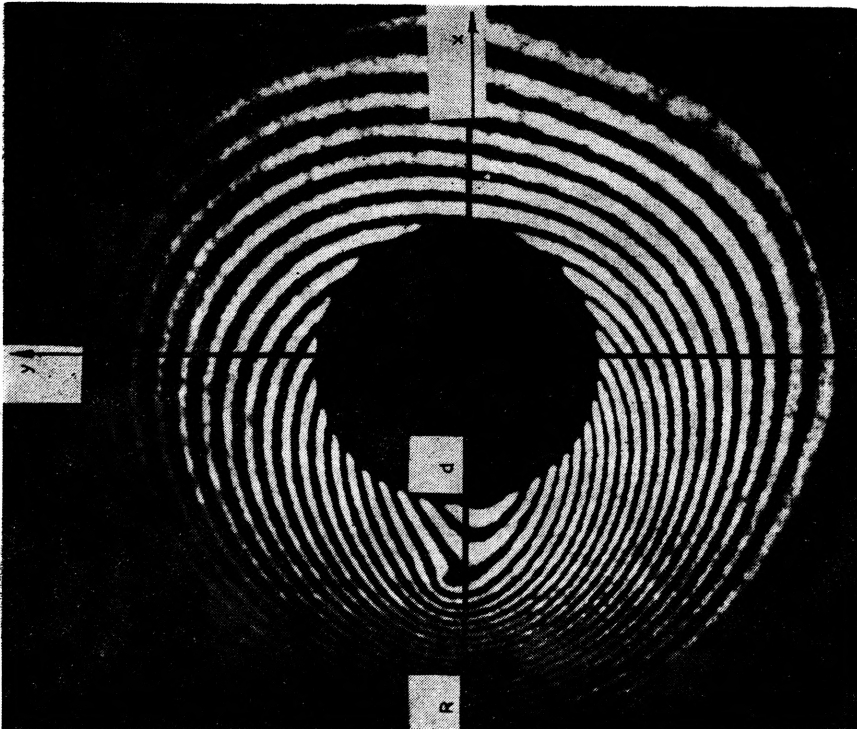
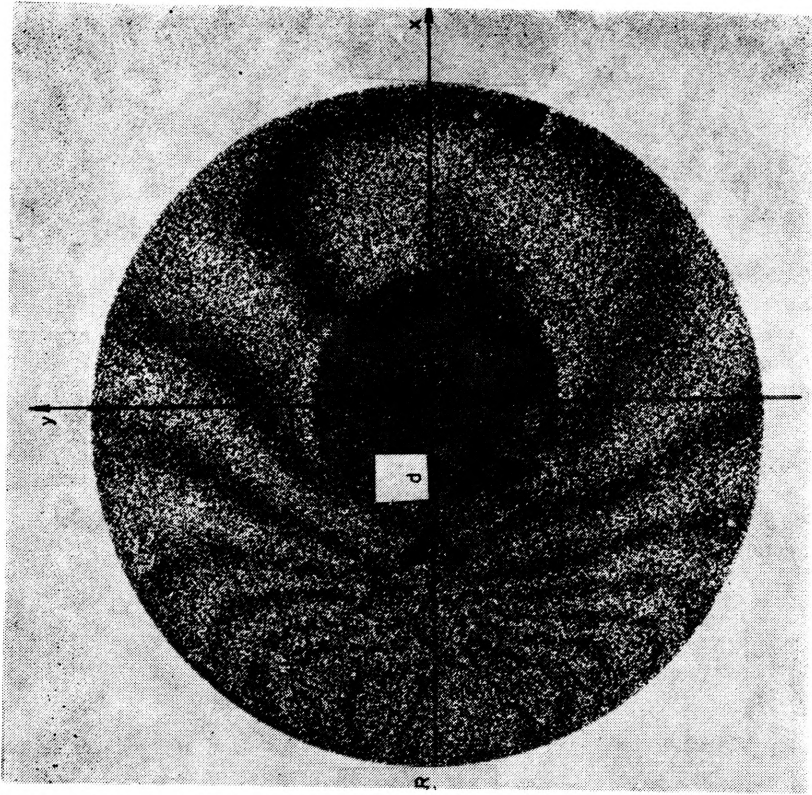


Fig. 4. The fringe patterns corresponding to the (a) holographic ($w \sim 4 \mu\text{m}$), (b) speckling ($w \sim 27 \mu\text{m}$) interferometry

For illustration two examples of interference patterns appearing in holographic and speckling interferometry, respectively, are given in Fig. 4. The holographic interferogram contains 19 fringes which indicates the bending of order of $4 \mu\text{m}$, while the speckling interferogram containing 6 fringes indicates the bending of about $27 \mu\text{m}$. When using the holographic method the last bending would produce the number of fringes which, being at the limit of resolving power of the eye, would be difficult to analyse.

References

- [1] ERF R., *Holographic Nondestructive Testing*, Academic Press, New York 1974.
- [2] ERF R., *Speckle Metrology*, Academic Press, New York 1978.
- [3] FU-PEN CHIANG, REN-MING JUANG, *Appl. Opt.* **15** (1976).
- [4] KHETAN R. P., CHIANG F. P., *Appl. Opt.* **15** (1976).

Received May 21, 1981

Imaging performance of angular and apodized aperture*

ANNA MAGIERA

Institute of Physics, Technical University of Wrocław, Wybrzeże Wyspiańskiego 27, 50-370 Wrocław, Poland.

1. Introduction

The complex degree of coherence is defined, according to VAN ZITTERT [1], by the normed Fourier transform of the source intensity function. In this case the source is represented by the diaphragm, the dimensions of which and optical field distribution are identical with those of the source. The intensity distribution in the source plane may be modified by introducing a central coverage. This leads to a one-dimensional change of the diffraction image of the source, i.e., an increase of the central coverage degree lowers the contrast and improves the resolution [2, 3]; this is the case in visualization of the objects in microscopy or in objective interferometry, for instance.

It is possible, moreover, to apply a programmed modification of the optical field by using an amplitude apodizer, i.e., by replacing the diaphragm-source by a profiled diaphragm and a cylindric lens [4]. The optical field of the source may be then modified by changing only the profile of the diaphragm. In this work the results obtained by applying both these methods are compared.

2. Coherence of the apodized source and the ring source

An extended circular and noncoherent source located in the (X_0, Y_0) plane and equivalent to the circle diaphragm of the radius (r) produces in the (X, Y) plane the partial coherence described by its complex degree μ_{12} :

* This work was carried on under the Research Project M.R. I.5.

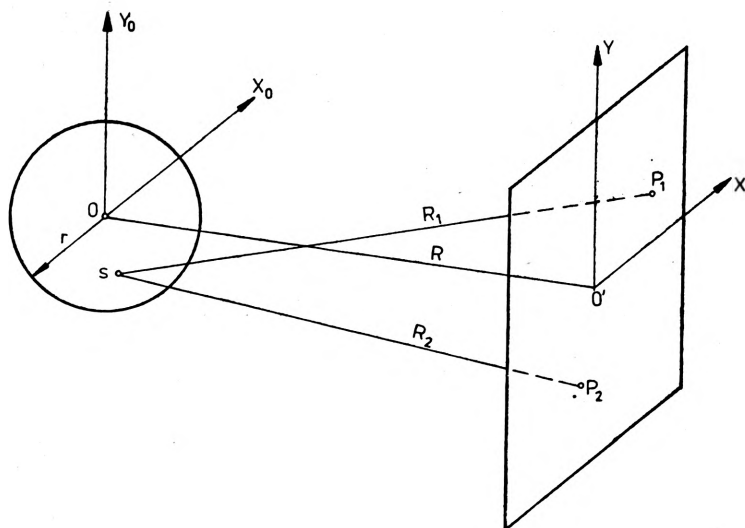


Fig. 1. Light source-diffraction plane

$$\mu_{12} = \frac{\exp(i\Psi) \iint_S I(X_0, Y_0) \exp\left[\frac{-2\pi i}{\lambda} (pX_0 + qY_0)\right] dX_0 dY_0}{\iint_S I(X_0, Y_0) dX_0 dY_0}, \quad (1)$$

where (X_0, Y_0) — coordinates of a point in the source plane (Fig. 1),

$I(X_0, Y_0)$ — light source intensity,

$$p = \frac{X_1 - X_2}{R}, \quad q = \frac{Y_1 - Y_2}{R},$$

(X_i, Y_i) — coordinates of the point in the diffraction image plane,

$$\Psi = \frac{2\pi}{\lambda} \left[\frac{(X_1^2 + Y_1^2) - (X_2^2 + Y_2^2)}{2R} \right].$$

For a uniform circular source of the radius (r) and transmittance $T(r) = 1$, under the condition $OP_1 - OP_2 \ll \lambda$ (Fig. 1), the formulae for the degree of partial coherence in the image plane may be written as

$$\mu_{12}(v) = \frac{2J_1(v)}{v}, \quad (2)$$

where $v = \frac{2\pi r}{\lambda} \sqrt{p^2 + q^2}$ — transversal shift.

The apodizer of transmittance $T(r) = 1 - r^2$ produces in the image plane the partial coherence described by the formula

$$\mu_{12}(v) = \frac{8}{v^2} \left[\frac{2J_1(v)}{v} - J_0(v) \right]. \quad (3)$$

Correspondingly, the apodizer of transmittance $T(r) = \frac{1}{2} (1+r^2)$ produces the degree of partial coherence given by:

$$\mu_{12}(v) = \frac{8}{3v} \left[J_1(v) - \frac{2}{v^2} J_1(v) + \frac{1}{v} J_0(v) \right], \quad (4)$$

while the apodizer of transmittance $T(r) = r^2$

$$\mu_{12}(v) = \frac{4}{v} \left[J_1(v) - \frac{4}{v^2} J_1(v) + \frac{2}{v} J_0(v) \right]. \quad (5)$$

The results are shown in Fig. 2. The respective distributions of the light intensities in the diffraction images of the sources are shown in Fig. 3. The part of energy (E) which is contained in the increasing regions (v) of the diffraction images, the centrum of which is the geometrical centre is shown in Fig. 4.

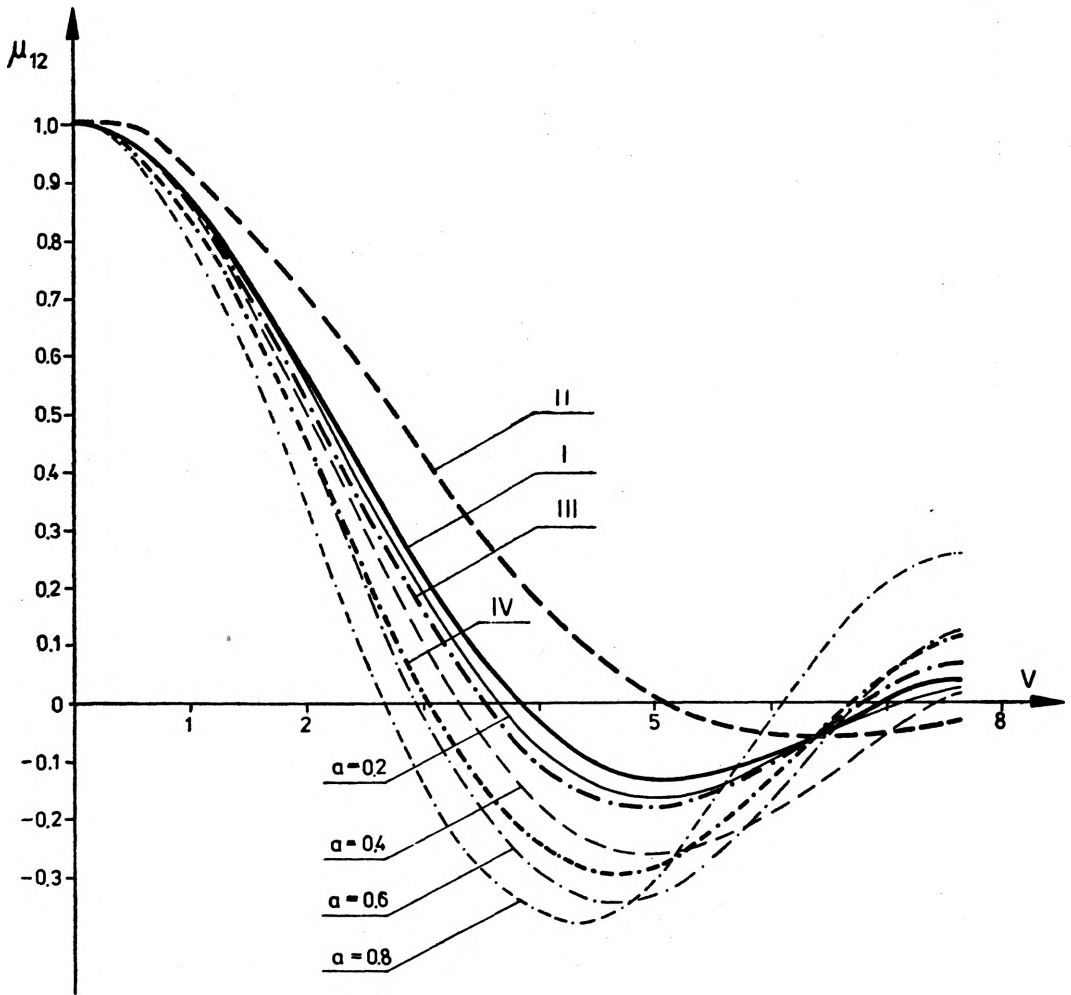


Fig. 2. Coherence of the apodized source of transmittance $T(r)$ and the uniform source of central coverage: α - radius of circular coverage normalized by the source radius. I - non-apodized, II - $1-r^2$, III - $\frac{1}{2}(1+r^2)$, IV - r^2

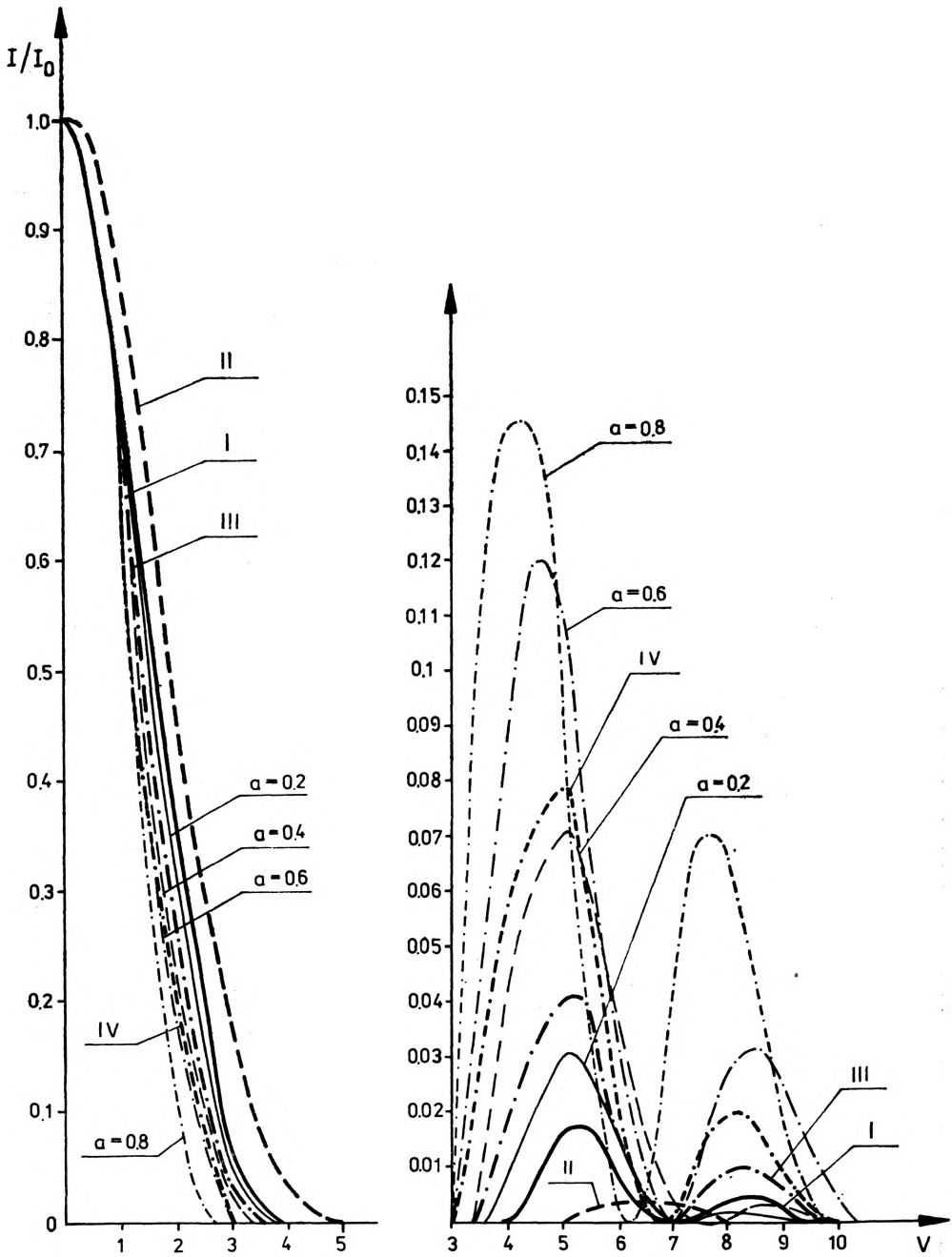


Fig. 3. The intensity distribution in the diffraction image of the apodized source and the ring source. I - non-apodized, II - $1-r^2$, III - $\frac{1}{2}(1+r^2)$, IV - r^2

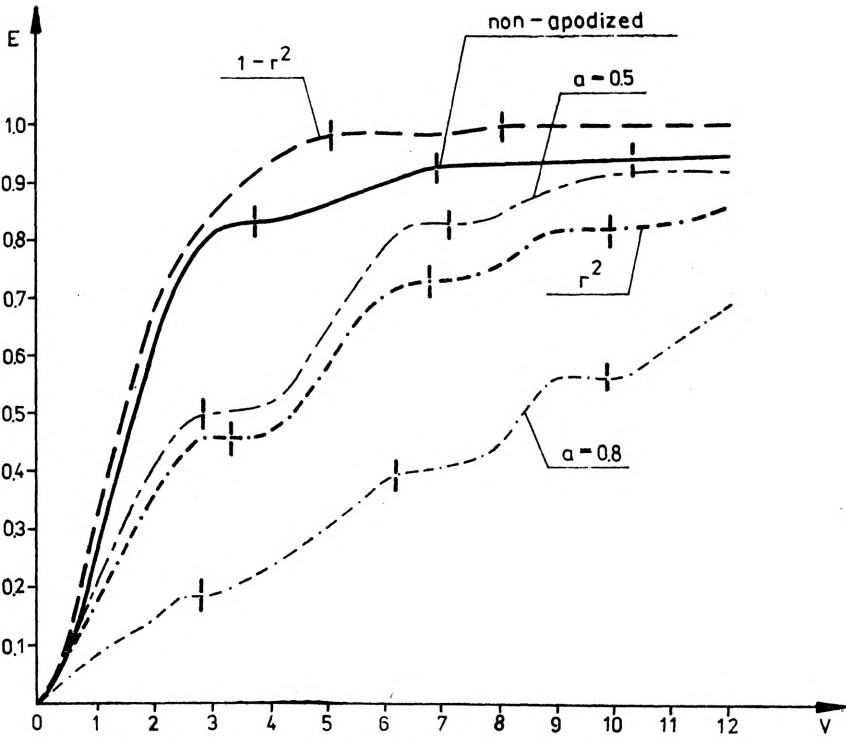


Fig. 4. The energy distribution in the increasing regions examined

Table. Coherent areas $P_1P_2 = \frac{v\lambda R}{2\pi r}$ for the apodized sources of transmittance $T(r)$ and for uniform sources covered centrally (a degree of coverage)

Source	$1-r^2$	1	$a = 0.2$	$\frac{1}{2}(1+r^2)$	$a = 0.4$	r^2	$a = 0.6$	$a = 0.8$
v	1.22	1	0.95	0.93	0.90	0.80	0.78	0.73
(P_1P_2)	0.194	0.159	0.151	0.148	0.143	0.127	0.124	0.116

Greater area of the object is coherent

Smaller area of the object is coherent

By assuming that for a uniform diaphragm of transmittance $T(r) = 1$ and of angular size $a = r/R$ the region illuminated coherently has the sizes $P_1P_2 = \frac{0.159R}{r}$, [1], the coherent areas have been determined for the remaining sources. The results are given in Table.

From these results it follows that the sources of transmittance $T(r) = r^2$ and $T(r) = \frac{1}{2}(1+r^2)$ act in the same directions as the uniform sources covered centrally, i.e., they cause a decrease of the coherence area as compared to those produced by the source of transmittance $T(r) = 1$. On the other hand, the apodizer of transmittance $T(r) = 1-r^2$ produces higher coherence than a uniform source.

3. Two-point resolution of Sparrow-type. Energy contrast

The result obtained has been verified by calculating numerically the Sparrow resolution for a two-point object and the energy contrast for a periodic object. In Fig. 5 the critical values (δ_0) of the distance between two object points have been shown as a function of the coherence degree. In Fig. 6 the energy contrast

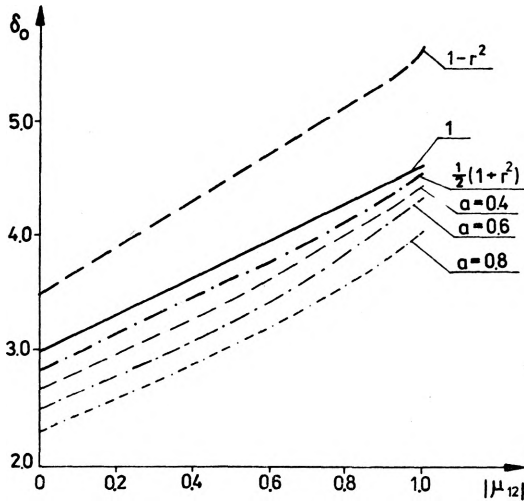


Fig. 5. Critical Sparrow distance (δ_0) between two-point objects for different source types

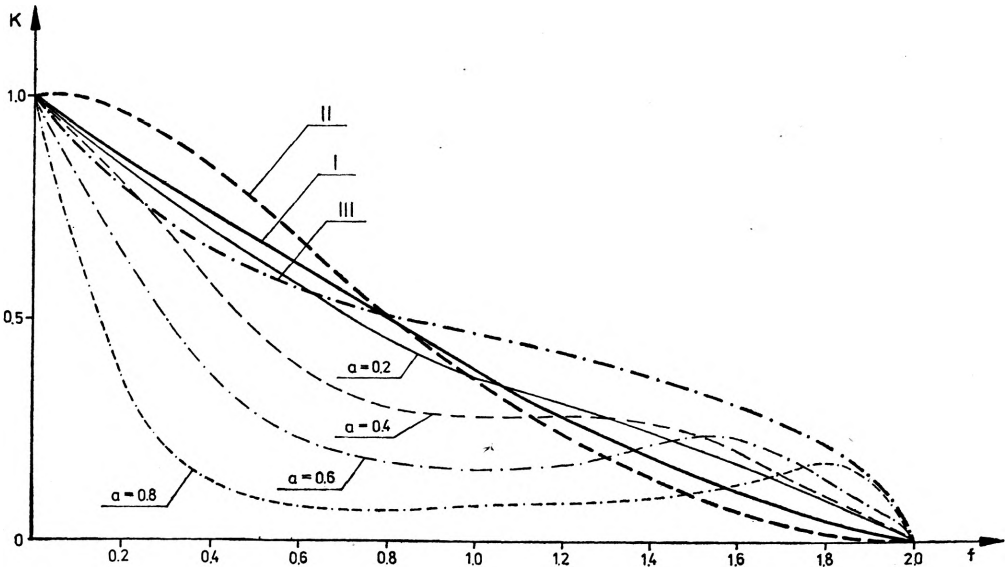


Fig. 6. Energy contrast of a cosinusoidal test of modulation depth equal to 0.5. I - non-apodized, II - $1-r^2$, III - $\frac{1}{2}(1+r^2)$

is shown for a periodic test of the modulation depth equal to 0.5. From the results obtained it may be seen that when the apodizers are used a stimulated modulation of the optical field is possible, which requires a solution of the respective optimization problem. An example of apodizing diaphragm profile determination for the required resolution is given in [5].

Similarly, by introducing an apodizer the contrast may be changed depending on the modulation depth in the object. This topic will be widely discussed in the work [6] prepared for publication.

References

- [1] BORN M., WOLF E., *Principles of Optics*, Ed. Nauka, Moskva 1973, p. 469 (in Russian).
- [2] ČANŽEK L., *Optik* **55** (1980), 371–384.
- [3] TŠHUNKO H. F. A., *Appl. Opt.* **13** (1974), 1820–1823.
- [4] MAGIERA A., PLUTA M., Non-Coherent Apodizing Simulator, *Optik* (in press).
- [5] MAGIERA A., *Optik* **55** (1980), 189–197.
- [6] MAGIERA A., PIETRASZKIEWICZ K., *Image Contrast of the Coherent Apodized Optical System* (in preparation).

Received June 11, 1981.